North Pacific Fisheries Commission

NPFC-2020-TWG CMSA03-WP05 (Rev.1)

Application of Virtual Population Analysis (VPA) and State-space Assessment Model (SAM) to the Shared Data of Chub Mackerel in the Northwest Pacific

Shota Nishijima, Ryuji Yukami, Kazuhiro Oshima, and Momoko Ichinokawa

Fisheries Resources Institute,

Japan Fisheries Research and Education Agency (FRA)

(corresponding author: Shota Nishijima, nishijimash@affrc.go.jp)

Summary

The Technical Working Group for Chub Mackerel Stock Assessment in NPFC has decided to use an operating model (OM) for comparing the performance of different four assessment model candidates. Japan has proposed tuned virtual population analysis (VPA) and state-space assessment model (SAM) as candidate stock assessment models. In this paper, we report the results on application of the two models to the merged data that has been shared among the members for OM development. Although the past estimates were close between VPA and SAM, the recent abundance estimates in VPA were greatly higher than those in the SAM and the recent fishing pressure was greatly lower in the VPA. Both models did not show serious retrospective biases and it is difficult to determine which model is better from this result. The simulation testing will be important for the choice of best stock assessment model and we should discuss specific scenario settings in the operating model framework.

Note: Working document submitted to the NPFC 3rd Meeting of Technical Working Group on Chub Mackerel Stock Assessment, 11–14 November 2020. Document not to be cited without author's permission.

Introduction

The Technical Working Group on Chub Mackerel Stock Assessment (TWG CMSA) in NPFC determined that (1) the candidates of stock assessment models (VPA, ASAP, KAFKA, and SAM) would be compared by an operating model, and (2) the operating model would be based on POPSIM-A (NPFC 2019). POPSIM-A uses a stock assessment model as an operating model and, therefore, input data are needed for the development of operating models by fitting stock assessment model candidates (Deroba et al. 2014). Members in TWG CMSA (China, Japan, and Russia) respectively submitted potentially available data of chub mackerel and the merged data was distributed to the members (Nishijima 2020). Japan has proposed tuned virtual population analysis (VPA) and state-space assessment model (SAM) as candidates (Nishijima et al. 2018). Here we applied the two candidate models to the merged data and showed the methods and results.

Model

Virtual population analysis

The VPA assumes no error in catch-at-age and conducts a backward calculation of population dynamics. We assumed that the age structure was from 0 to 6+ and used the Pope's approximation (Pope 1972) to estimate fish numbers and fishing mortality coefficients:

$$N_{a,y} = N_{a+1,y+1} \exp(M_a) + C_{a,y} \exp\left(\frac{M_a}{2}\right), \qquad \text{if } a \le 4 \qquad (1)$$

$$N_{5,y} = \frac{C_{5,y}}{C_{5,y} + C_{6+,y}} N_{6+} \exp(M_5) + C_{5,y} \exp\left(\frac{M_5}{2}\right), \qquad (2)$$

$$N_{6+,y} = \frac{C_{6+,y}}{C_{5,y} + C_{6+,y}} N_{6+} \exp(M_6) + C_{6+,y} \exp\left(\frac{M_6}{2}\right), \qquad (3)$$

where $N_{a,y}$ is the fish number at age a in year y and $C_{a,y}$ is the catch at age at age a in year y, and M_a is the natural mortality coefficients at age a. We here used $M_a = 0.41$ for all age classes because this value was the median of various M estimators (Takahashi et al. 2018). The fish numbers in the terminal year (2019) was calculated from the fishing morality coefficients in the terminal year:

$$N_{a,2019} = \frac{C_{a,2019} \exp\left(\frac{M_a}{2}\right)}{1 - \exp\left(-F_{a,2019}\right)}. \qquad (4)$$

The fishing mortality coefficients except for the terminal year were computed from

$$F_{a,y} = -\log\left\{1 - \frac{C_{a,y}}{N_{a,y}} \exp\left(\frac{M_a}{2}\right)\right\} . \tag{5}$$

We also assumed that the fishing mortality coefficient of plus group (A+) were identical to that of A−1:

$$F_{6+,y} = F_{5,y} . \tag{6}$$

We used ‘ridge VPA’ to stabilize the terminal F estimates, which included a ridge penalty (squared term of estimated parameters) in the optimization, i.e., penalized likelihood (Okamura et al. 2017):

$$\text{minimize} \quad (1-\lambda) \sum_k \sum_y \left[\frac{\ln(2\pi v_k^2)}{2} + \frac{\left\{\ln(I_{k,y}) - \ln(q_k X_{k,y}^{b_k})\right\}^2}{2v_k^2}\right] + \lambda \sum_{a=0}^{5} F_{a,2019}^2 , \tag{7}$$

where λ is the penalty coefficient ($0 \le \lambda < 1$), $I_{k,y}$ is the value of index k in year y, v_k^2 is the variance of index k, q_k is the proportionality constant, and b_k is the nonlinear coefficient between index k and its associated estimates X_k. We used the four indices from Japan (fleet no.2-5), because their association with abundance estimates are clear (two for recruitment and two for SSB), whilst the usages of other members’ indices are unclear (Nishijima et al. 2020). We estimated $b_{k,y}$ to treat hyperstability or hyperdepletion. We selected the penalty coefficient (λ = 0.85) so as to minimize the absolute value of Mohn’s rho (Mohn 1999) of average fishing mortality coefficient in the five-year retrospective analysis:

$$\rho = \frac{1}{5} \sum_{i=1}^{5} \left(\frac{\hat{F}_{2019-i}^{R} - \hat{F}_{2019-i}}{\hat{F}_{2019-i}}\right), \tag{8}$$

where $\hat{F}_{2019-i}$ is the estimate of average fishing mortality coefficients in year 2019−i using the full data and $\hat{B}_{2019-i}^{R}$ is the corresponding estimate when removing the data after 2019−i. Therefore, the ridge VPA can reduce a retrospective bias to some extent.

State-space assessment model

The basic model structure of SAM followed the original one (Nielsen and Berg 2014). Numbers at age a in year y are described as:

$$\log(N_{0,y}) = \log(N_{0,y-1}) + \eta_{0,y}, \tag{9}$$

$$\log(N_{a,y}) = \log(N_{a-1,y-1}) - F_{a-1,y-1} - M_{a-1,y-1} + \eta_{a,y}, \qquad 1 \le a \le 5 \quad (10)$$

$$\log(N_{6+,y}) = \log\left(N_{5,y-1}e^{-F_{5,y-1}-M_{5,y-1}} + N_{6+,y-1}e^{-F_{6+,y-1}-M_{6+,y-1}}\right) + \eta_{6+,y}\,, \quad (11)$$

where $\eta_{a,y}$ is the process error at age a in year y. We assumed different magnitudes of the process errors for age 0 and older: $\eta_{0,y} \sim N(0, \omega_R^2), \eta_{a,y} \sim N(0, \omega_{S,a}^2)$ $(a > 0)$. We fixed the variance for the ages older than 0 at a small value ($\omega_{S,a}^2 = 0.0001$) because of a failure to converge when estimating this parameter.

The fishing mortality coefficient was assumed to follow the multivariate random walk:

$$\log(\boldsymbol{F_y}) = \log(\boldsymbol{F_{y-1}}) + \boldsymbol{\xi}_y\,, \qquad \text{if } y \neq 2011 \quad (12)$$

where $\boldsymbol{F_y} = (F_{1,y}, \ldots, F_{A+,y})^T$, $\boldsymbol{\xi_y} \sim \mathrm{MVN}(0, \boldsymbol{\Sigma})$, and $\boldsymbol{\Sigma}$ is the variance-covariance matrix of multivariate normal distribution (MVN). The diagonal elements of matrix $\boldsymbol{\Sigma}$ were σ_a^2, while off-diagonal elements were assumed to be $\rho^{|a-a'|}\sigma_a\sigma_{a'}$ $(a \neq a')$. $\rho^{|a-a'|}$ corresponded to the correlation coefficient of F between ages a and a', and this assumption reflected the decrease in correlation with increasing age difference. In addition, we assumed $F_{6+,y} = F_{5,y}$ in accordance with tuned VPA. The random walk was omitted in 2011 because the fishing effort on chub mackerel possibly greatly decreased since the previous year because of the Great East Japan Earthquake and tsunami in March 2011. We found positive retrospective bias in stock abundance and negative bias in fishing mortality if assuming a random walk in 2011 (Fig. 1).

The SAM estimated the errors in catch-at-age in a lognormal fashion:

$$\log(C_{a,y}) = \log\left(\frac{F_{a,y}}{F_{a,y} + M_{a,y}}\left(1 - \exp(-F_{a,y} - M_{a,y})\right)N_{a,y}\right) + \varepsilon_{a,y} \quad (13)$$

where $\varepsilon_{a,y} \sim \mathrm{N}(0, \tau_a^2)$. We used the four indices from Japan in the same way as the VPA:

$$\log(I_{k,y}) = \log(q_r X_y^{b_k}) + \eta_{k,y}\,, \quad (14)$$

where $\eta_{k,y}$ is the measurement error of index k in year y: $\eta_{k,y} \sim N(0,\ \nu_k^2)$.

The SAM has to estimate many parameters. We then imposed the following limitations to stability estimation and avoid overfitting:

$$\omega_{S,a} = \omega_S \ \left(\forall a\ (a > 0)\right), \quad (15)$$

$$\sigma_0 = \sigma_1,\ \sigma_2 = \sigma_3 = \cdots = \sigma_A\,, \quad (16)$$

$$\tau_2 = \tau_3, \ \tau_5 = \tau_{6+}. \tag{17}$$

These limitations were determined based on the Akaike information criteria (AIC).

In contrast to VPA, SAM regard state variables, such as numbers at age and *F* at age, as latent random variables, which requires complex, difficult numerical integral calculation for many random effects. We therefore used Template Model Builder (TMB: Kristensen, Nielsen, Berg, Skaug, & Bell, 2016), an R package which enables fast computation for latent variable models. We also made bias correction of mean values because random effects were estimated by logarithmic scale (Thorson and Kristensen 2016).

Stock-recruitment relationship and MSY reference point

We estimated the Hockey-Stick (HS) stock-recruitment relationship using estimated spawning stock biomass and the number of recruits. We used the HS relationship because we have used this stock-recruitment relationship in the domestic stock assessment. The HS relationship is useful to a feasible biological reference points based on maximum sustainable yield (MSY) when the stock has an extreme stock-recruitment relationship, i.e., too low or high steepness (Ichinokawa et al. 2017). We deterministically calculated MSY-based reference points using biological parameters (natural mortality coefficient, maturity at age, and weight at age) in recent five years (2015-2019). We then described a Kobe plot that shows the status of fishing impacts and spawning stock biomass.

Sensitivity analyses

We conducted two kinds of sensitivity analyses to examine the effects of data uncertainties and model assumptions. First, we analyzed the SAM with the Beverton-Holt relationship (Appendix A). Second, we analyzed VPA and SAM with age-specific natural mortality coefficients (Appendix B). Both results are shown in Appendices.

Results and Discussion

Although the past estimates of biomass, SSB, and recruitment were close between VPA and SAM, the recent abundance estimates were greatly higher in the VPA than those in the SAM (Figs. 2, 3). The fishing mortality coefficients of VPA in recent years were oppositely lower than those of SAM (Figs. 2, 3). The percent SPR corresponding to the fishing mortality for the most recent five years (2015-2019) was 54.4% on average (44.38-65.23%) in VPA, but 39.6% on average (35.9-48.0%) in the SAM. Accordingly, the SAM obtained more pessimistic results than the VPA. In addition, the uncertainties in recent estimates were much larger in the VPA than in the SAM (Fig. 3). The selectivity was highly variable in the VPA, but this variability was smoothed in the SAM (Fig. 4). The SAM estimated a larger variance of fishing mortality process (σ_a^2) at ages 0 and 1 than that at older ages and a strong correlation between neighbor ages (Table 1).

The difference of estimates between models can be explained by the fitting pattern of tuning indices. For the recruitment indices the nonlinear coefficients (b_k) were lower in the VPA than in the SAM, although the magnitudes of measurement errors (ν_k) little differed (Table 2). This causes the recruitment estimates in recent years higher in the VPA than in the SAM (Fig. 5). Especially, the VPA fitted better to the highest values of recruitment indices in 2018 than the SAM (Figs. 6-7), causing the extremely strong year classes of 2018 (Figs 2-3). On the other hand, the fitting to SSB indices was better in the SAM than in the VPA (Table 1, Fig. 5). Moreover, the recent SSB estimates in the VPA were higher than expected from the indices (Fig. 6) and the higher autocorrelation of residuals was found in the VPA than in the SAM (Fig. 7). It is noteworthy that the SSB indices peaked out in recent three or five years (Fig. 5). However, the VPA showed a worse fitting to the SSB indices and estimated a continuous increase in SSB (Figs. 2-3). This worse fitting in the VPA was partly because the ridge penalty impaired the fitting instead of improved retrospective bias. In contrast to the deterministic calculation of fish population dynamics under the assumption of no error in catch-at-age, however, SAM estimates observation errors in catch-at-age (Figs. 8-9) and process errors in population dynamics, which can improve the fitting of indices in comparison to VPA. As a result, the VPA estimates were greatly affected by the recruitment indices, whereas the SAM estimates were greatly affected by the SSB indices, leading to the lower abundances and higher fishing impacts in the SAM than in the VPA.

Both models did not show serious retrospective biases in the estimates of abundances and fishing mortality (Figs. 10-11). Thus, the retrospective analysis did not inform us of inferior-to-superior relationship between SAM and VPA, although the estimated values were quite different.

Estimated HS relationships were quite different between VPA and SAM because the shape of HS relationship in VPA was largely affected by the extremely high values of SSB in the latest two years (Fig. 12). However, the steepness was estimated at around 0.70 for both models (Table 3). Although the absolute values of MSY reference points (MSY, SSB_{MSY}, and B_{MSY}) were much higher in the VPA than in the SAM because of the different HS relationships, the relative values of MSY-reference points to B0 (virgin stock) reference points (%SPR_{MSY}, SSB_{MSY}/SB0) were robust between the models (Table 3). Kobe plots were a bit different between models; SSB exceeded SSB_{MSY} only in the latest two years in the VPA, whereas SSB was also higher than SSB_{MSY} not only in the latest three years but also the 1970s for the SAM (Figs. 13-14). Both models estimated to be not overfishing ($F < F_{MSY}$) nor overfished ($SSB > SSB_{MSY}$) in the latest year (2019).

NPFC TWG-CMSA has determined that the choice of stock assessment model will be committed to the operating model using POPSIM-A (NPFC 2019). We will be able to simply generate simulation data from the fitting of data in both models, because the POPSIM-A uses a stock assessment model as an operating model (Deroba et al. 2014). For SAM, the simulated data on abundance indices and catch-at-age are generated from the equations 12 and 13. For VPA, however, the catch-at-age data is assumed to be correct and has no need to simulate; only the data of abundance indices should be simulated.

SAM can be extended to a model that allows multi-fleets and missing values, which is an advantage. However, VPA cannot deal with multi-fleets and, therefore, we should consider how to use multi-fleet data in the cross testing in which simulation and assessment models are different (Deroba et al. 2014). We should determine specific approaches and scenario settings to facilitate the stock assessment of chub mackerel in the Northwestern Pacific Ocean.

References

Deroba, J. J., D. S. Butterworth, R. D. Methot, J. A. A. DeOliveira, C. Fernandez, A. Nielsen, S. X. Cadrin, M. Dickey-Collas, C. M. Legault, J. Ianelli, J. L. Valero, C. L. Needle, J. M. O'Malley, Y. J. Chang, G. G. Thompson, C. Canales, D. P. Swain, D. C. M. Miller, N. T. Hintzen, M. Bertignac, L. Ibaibarriaga, A. Silva, A. Murta, L. T. Kell, C. L. DeMoor, A. M. Parma, C. M. Dichmont, V. R. Restrepo, Y. Ye, E. Jardim, P. D. Spencer, D. H. Hanselman, J. Blaylock, M. Mood, and P. J. F. Hulson. 2014. Simulation testing the robustness of stock assessment models to error: Some results from the ICES strategic initiative on stock assessment methods. ICES Journal of Marine Science 72:19–30.

Hashimoto, M., S. Nishijima, R. Yukami, C. Watanabe, Y. Kamimura, S. Furuichi, M. Ichinokawa, and H. Okamura. 2019. Spatiotemporal dynamics of the Pacific chub mackerel revealed by standardized abundance indices. Fisheries Research 219:105315.

Ichinokawa, M., H. Okamura., H. Kurota. 2017. The status of Japanese fisheries relative to fisheries around the world. ICES Journal of Marine Science 74: 1277–1287.

Kristensen, K., A. Nielsen, C. W. Berg, H. Skaug, and B. M. Bell. 2016. TMB: Automatic differentiation and laplace approximation. Journal of Statistical Software 70:1–21.

Mohn, R. 1999. The retrospective problem in sequential population analysis: An investigation using cod fishery and simulated data. ICES Journal of Marine Science 56:473–488.

Nielsen, A., and C. W. Berg. 2014. Estimation of time-varying selectivity in stock assessments using state-space models. Fisheries Research 158:96–101.

Nishijima, S. 2020. Compilation and summary of shared data for operating models of the chub mackerel in the Northwestern Pacific. NPFC-2020-TWG CMSA03-WP04.

NPFC 2019. 2nd Meeting of the Technical Working Group on Chub Mackerel Stock Assessment. 2019. 2nd Meeting Report. NPFC-2019-TWG CMSA02-Final Report. (available at www.npfc.int)

Okamura, H., Y. Yamashita, and M. Ichinokawa. 2017. Ridge virtual population analysis to reduce the instability of fishing mortalities in the terminal year. ICES Journal of Marine Science 74:2427–2436.

Pope, J. G. 1972. An investigation in the accuracy of the virtual population analysis using cohort analysis. ICNAF Research Bulletin 9:65–74.

Takahashi, N., Y. Kamimura, Y., M. Ichinokawa, S. Nishijima, R. Yukami, C. Watanabe, and H. Okamura 2018. A range of estimates of natural mortality rate for chub mackerel in the North Pacific Ocean. NPFC-2019-TWG-CMSA02-WP01.

Thorson, J. T., and K. Kristensen. 2016. Implementing a generic method for bias correction in statistical models using random effects, with spatial and population dynamics examples. Fisheries Research 175:66–74.

Tables

Table 1: Estimates of parameters of fixed effects in VPA and SAM. Parameter estimates associated with abundance indices are shown in Table 2.

Parameter	Not age-specific	Age (a) 0	1	2	3	4	5	6+
	VPA							
F_{2019}	-	0.09	0.01	0.05	0.03	0.13	0.37	0.37
	SAM							
σ_a	-	0.44	0.44	0.32	0.32	0.32	0.32	0.32
ρ	0.92	-	-	-	-	-	-	-
ω_a	-	0.73	0.01	0.01	0.01	0.01	0.01	0.01
τ_a	-	0.88	0.63	0.30	0.30	0.43	0.69	0.69

Table 2: Estimates of parameters associated with the abundance indices in VPA and SAM.

Fleet	q_k VPA	q_k SAM	b_k VPA	b_k SAM	υ_k VPA	υ_k SAM
2	6.90×10^{-6}	5.05×10^{-7}	1.22	1.60	1.17	1.23
3	1.01×10^{-7}	2.27×10^{-8}	1.38	1.92	0.77	0.82
4	5.93×10^{-6}	5.83×10^{-7}	0.78	1.10	0.73	0.59
5	5.04×10^{-5}	2.65×10^{-4}	0.45	0.63	0.31	0.31

Table 3: MSY-based reference points for different models and stock-recruitment relationship.

Model	SR	Reference	Catch (1000 ton)	Biomass (1000 ton)	SSB (1000 ton)	Exploit. rate	SPR0	Steepness
VPA	HS	MSY	1836	9250	3270	0.20	69	0.70
		B0	0	17985	11047	0.00	443	-
		MSY2B0	-	0.51	0.30	-	0.16	-
SAM (RW)*	HS	MSY	573	2969	1072	0.19	77	0.69
		B0	0	5675	3486	0.00	443	-

		MSY2B0	-	0.52	0.31	-	0.17	-
SAM (BH)§	**BH**	MSY	2283	24450	12085	0.09	79	0.44
		B0	0	51292	31507	0.00	443	-
		MSY2B0	-	0.48	0.38	-	0.18	-

* RW means the random walk of recruitment process

§ BH means the Beverton-Holt stock-recruitment relationship whose results are shown in Appendix A.

Figures

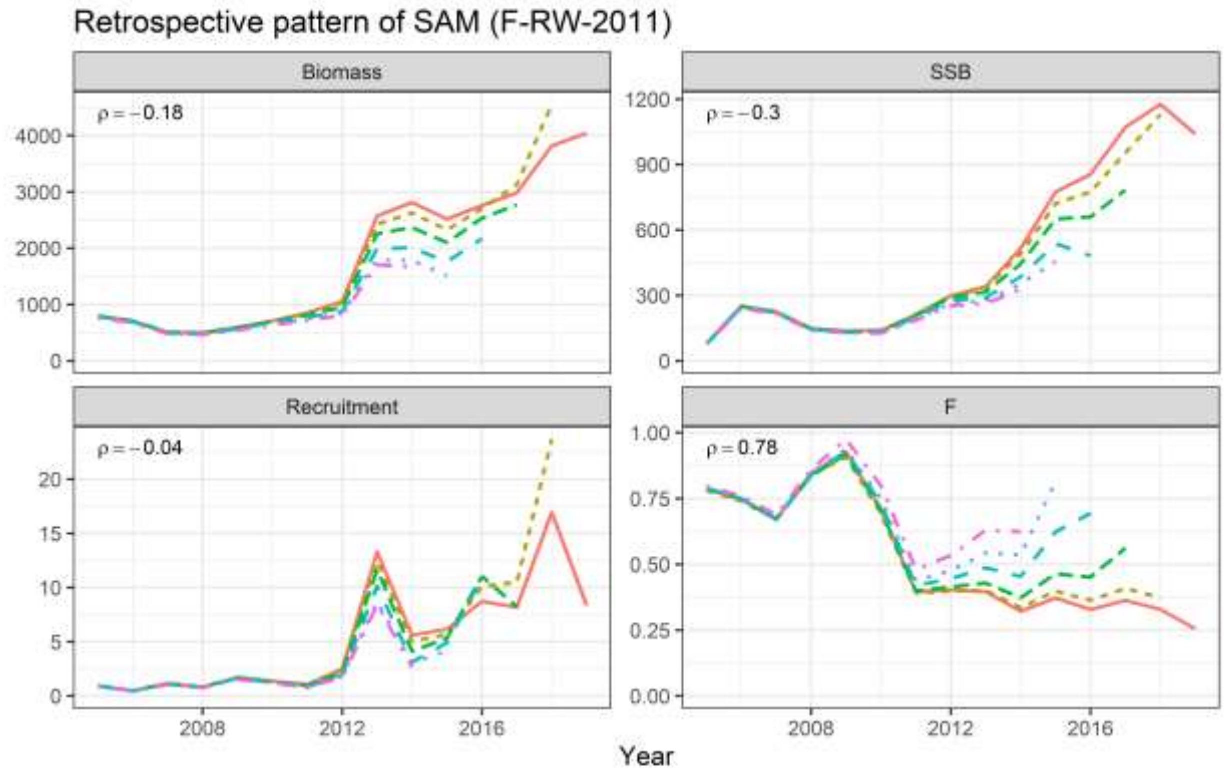

Figure 1: Retrospective pattern of SAM assuming the random walk of fishing mortality coefficients in 2011. Mohn's rho is shown in the upper-left side.

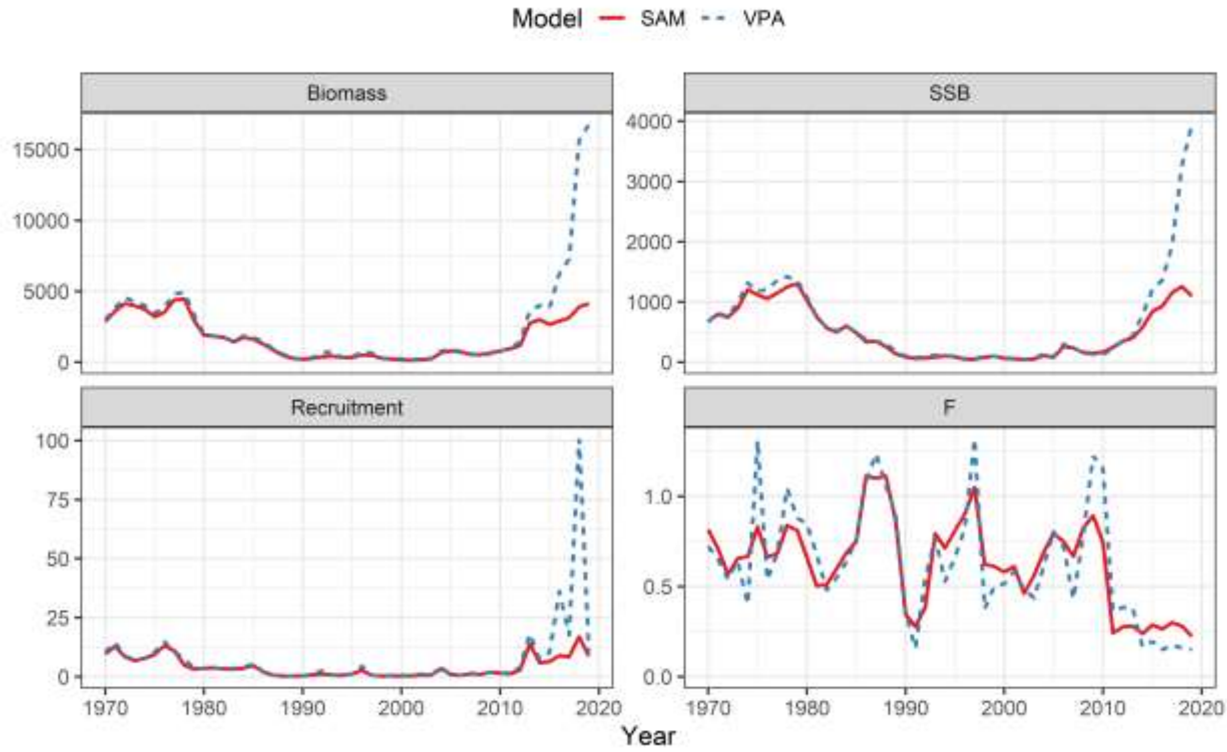

Figure 2: Time series of estimates of total biomass (thousand ton), SSB (thousand ton), recruitment (billion), and average fishing mortality coefficient of SAM and VPA. Confidence intervals are omitted from this figure because the intervals in the latest year of VPA are too large to plot (see Fig. 3).

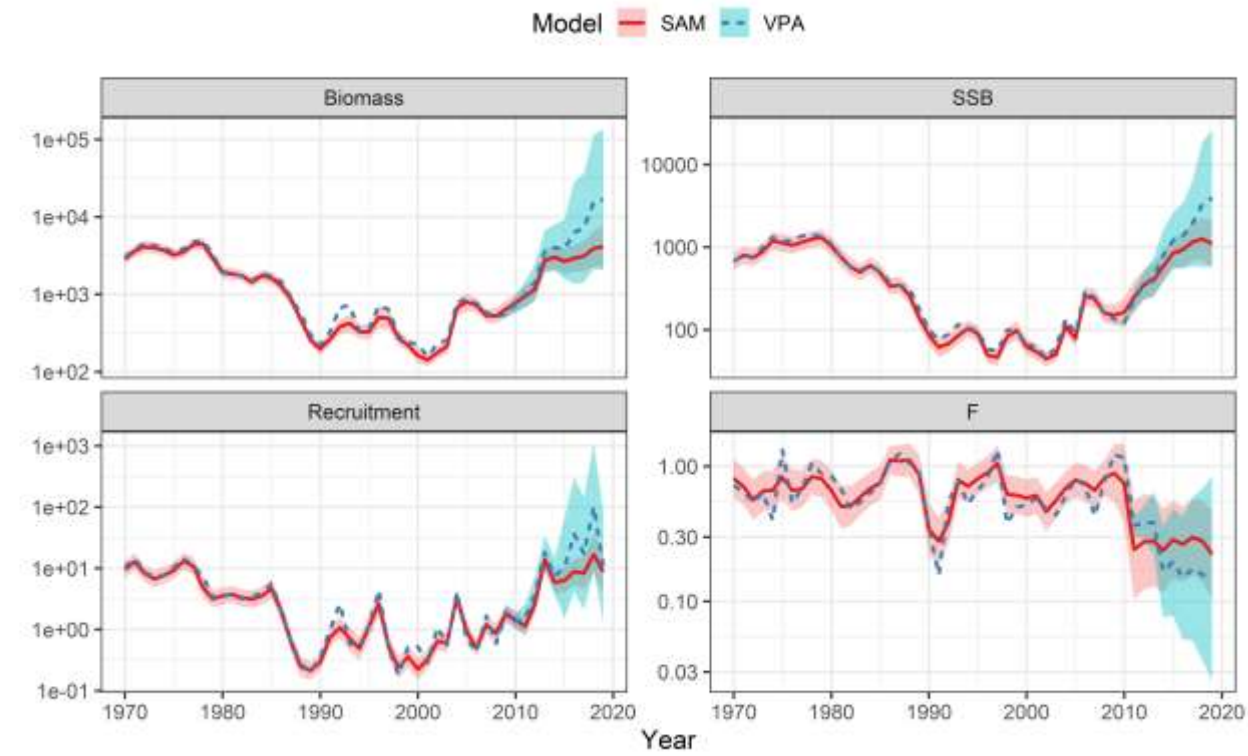

Figure 3: Time series of estimates of total biomass (thousand ton), SSB (thousand ton), recruitment (billion), and average fishing mortality coefficient of SAM and VPA at logarithmic scale. The shadows represent 95% confidence intervals estimated from the delta method.

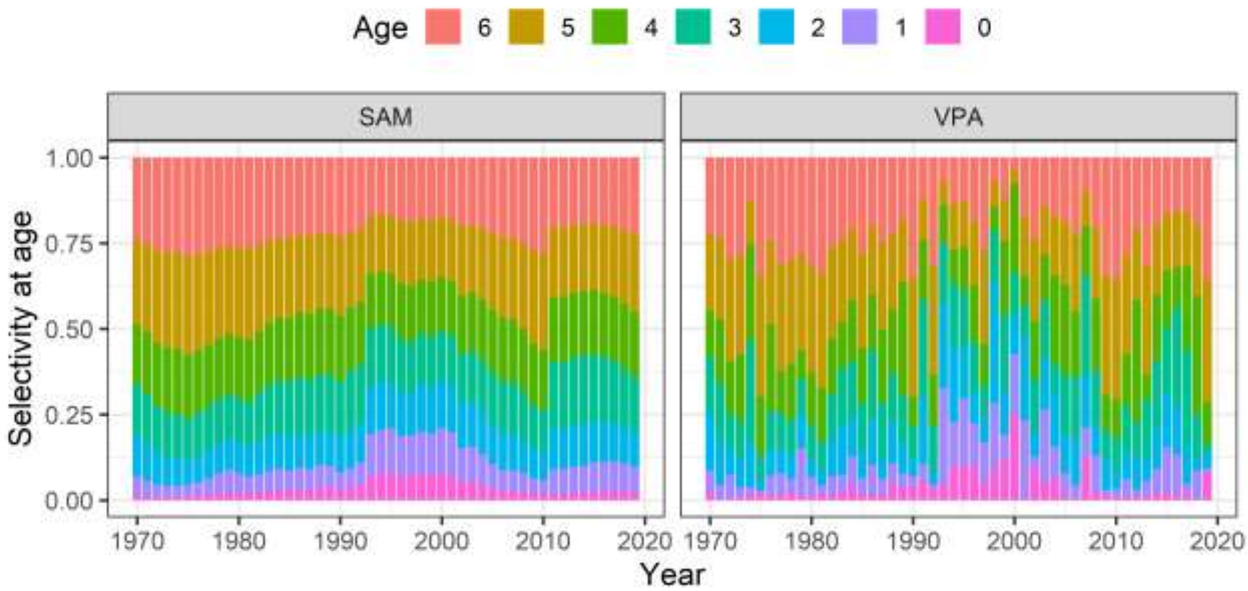

Figure 4: Time series of selectivity estimates of SAM (left) and VPA (right). Selectivity is scaled so that the total value is equal to one.

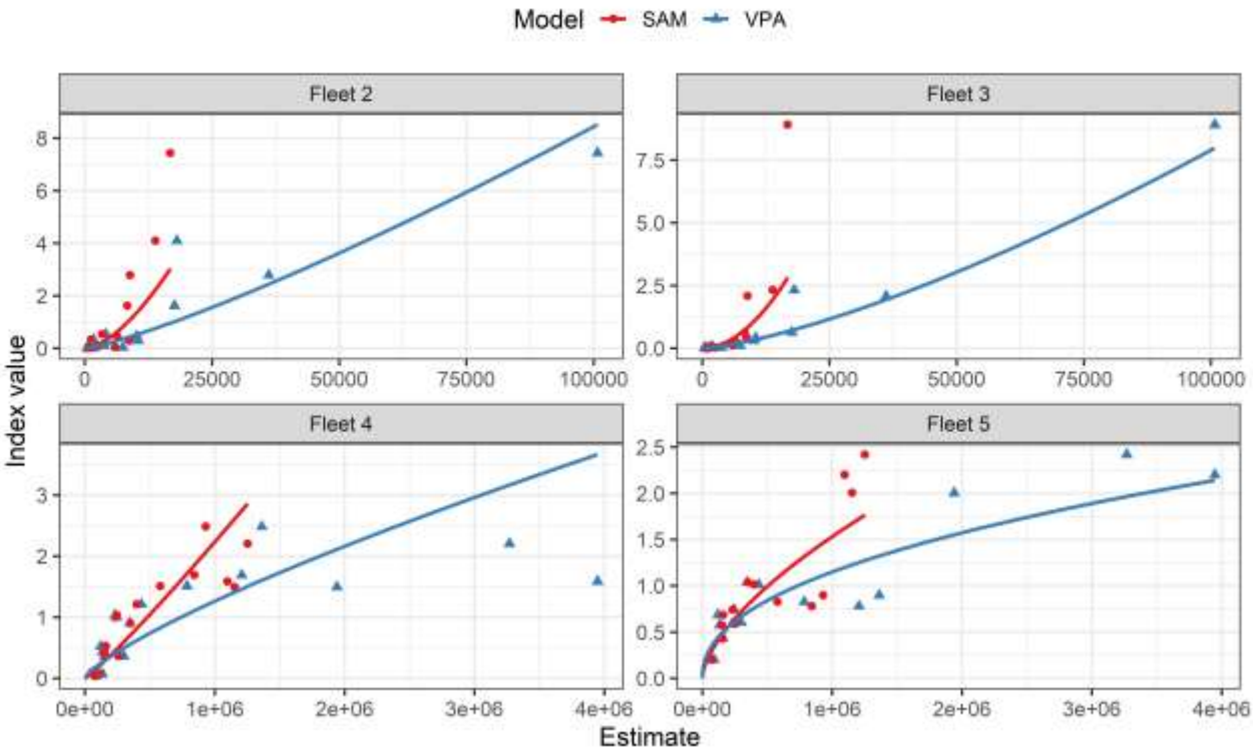

Figure 5: Relationships between indices and corresponding estimates in SAM (red circles, lines) and VPA (blue triangles, lines).

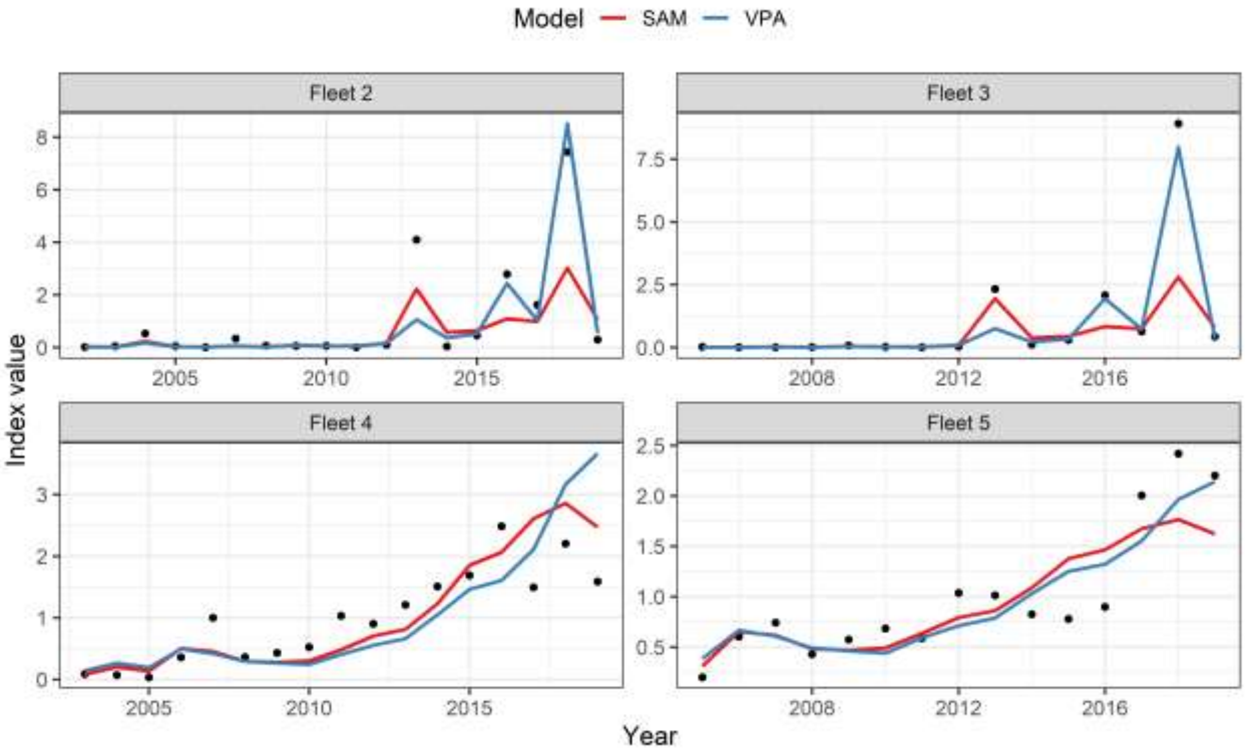

Figure 6: Time series of indices (points) and predictions by SAM (red lines) and VPA (blue lines).

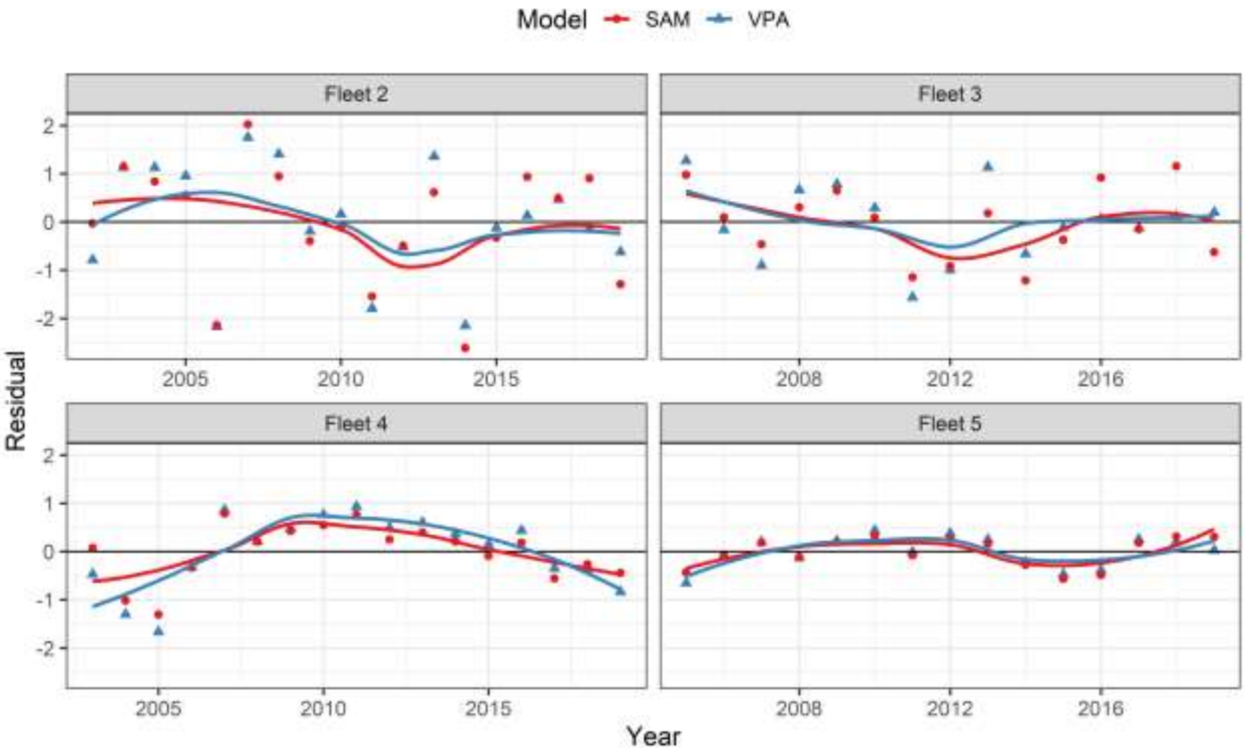

Figure 7: Time series of index residuals in SAM (red circles) and VPA (blue triangles). Smoothed curves are shown.

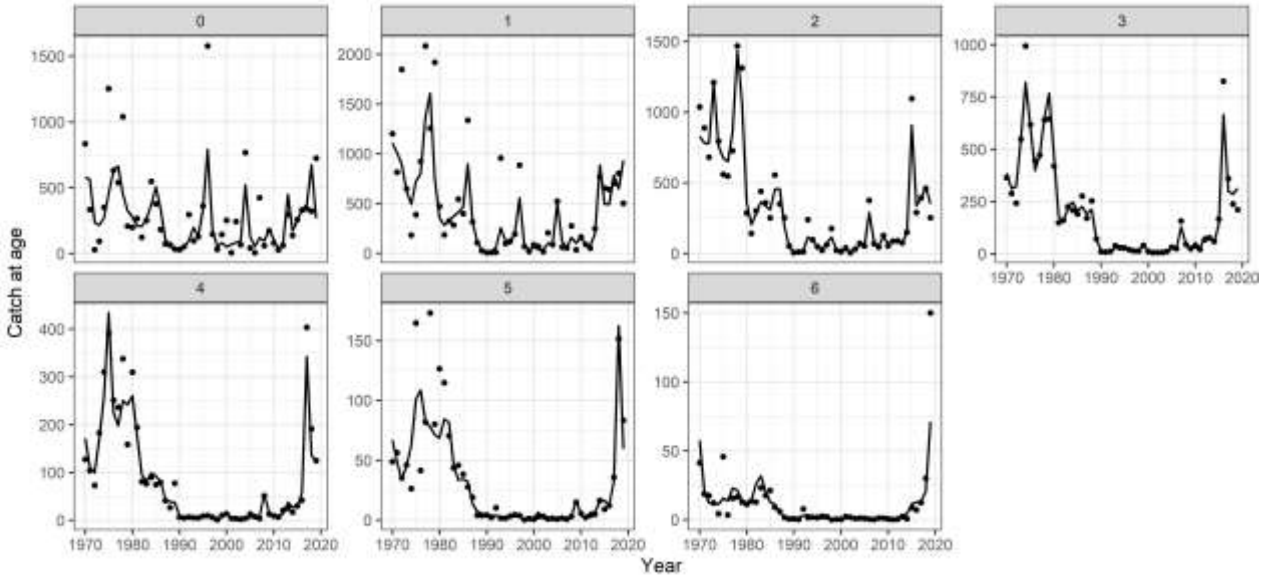

Figure 8: Time series of observed (points) and predicted values (points) of catch-at-age in SAM.

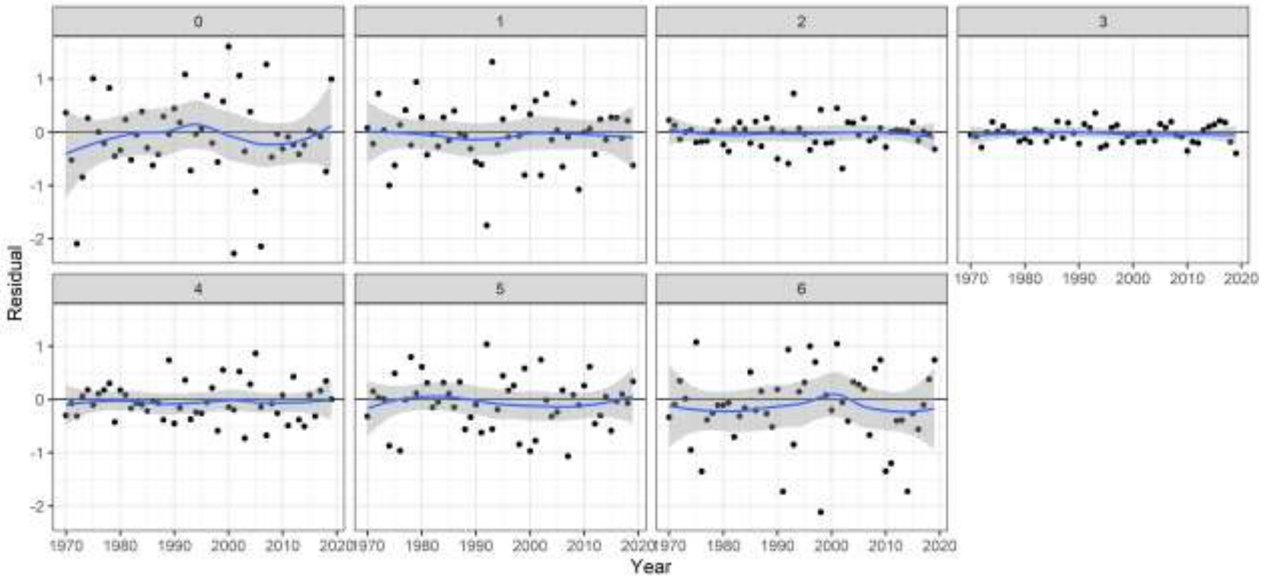

Figure 9: Time series of residuals between orbserved and predicted values of catch-at-age in SAM. Smoothed curves are shown with 95% confidence intervals.

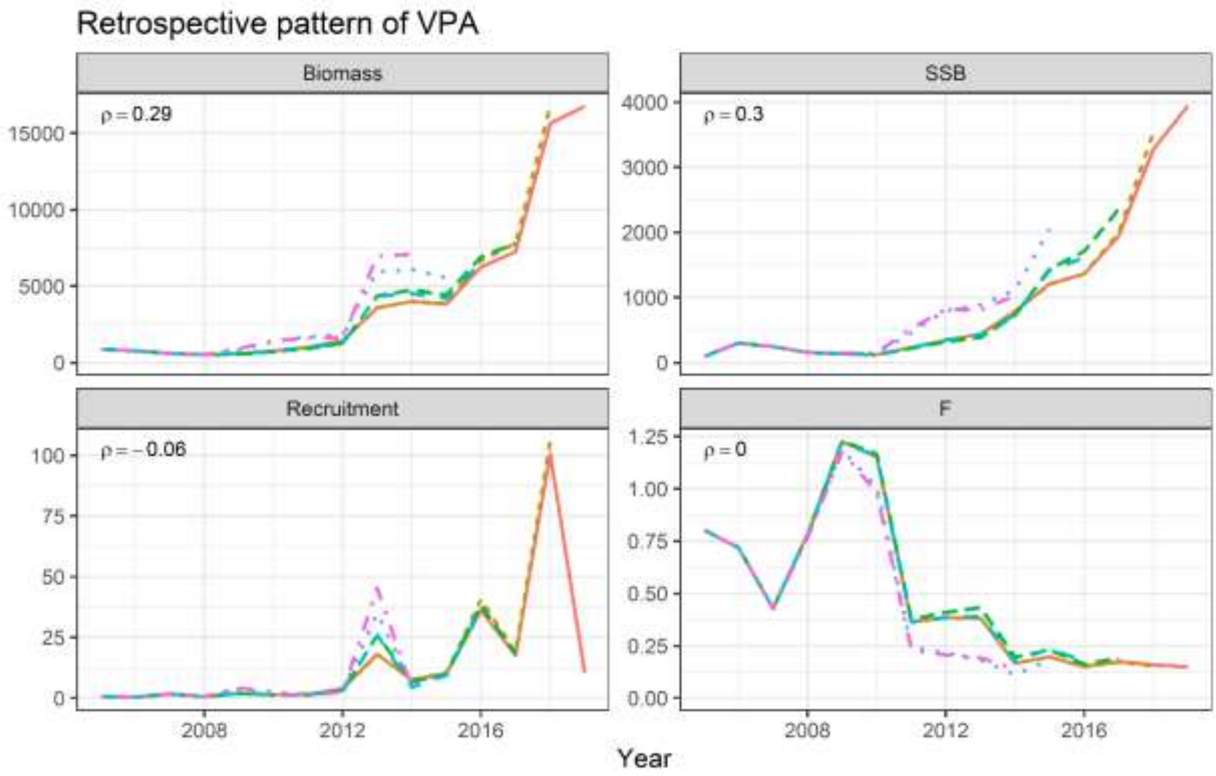

Figure 10: Retrospective pattern of VPA. Mohn's rho is shown in the upper-left side.

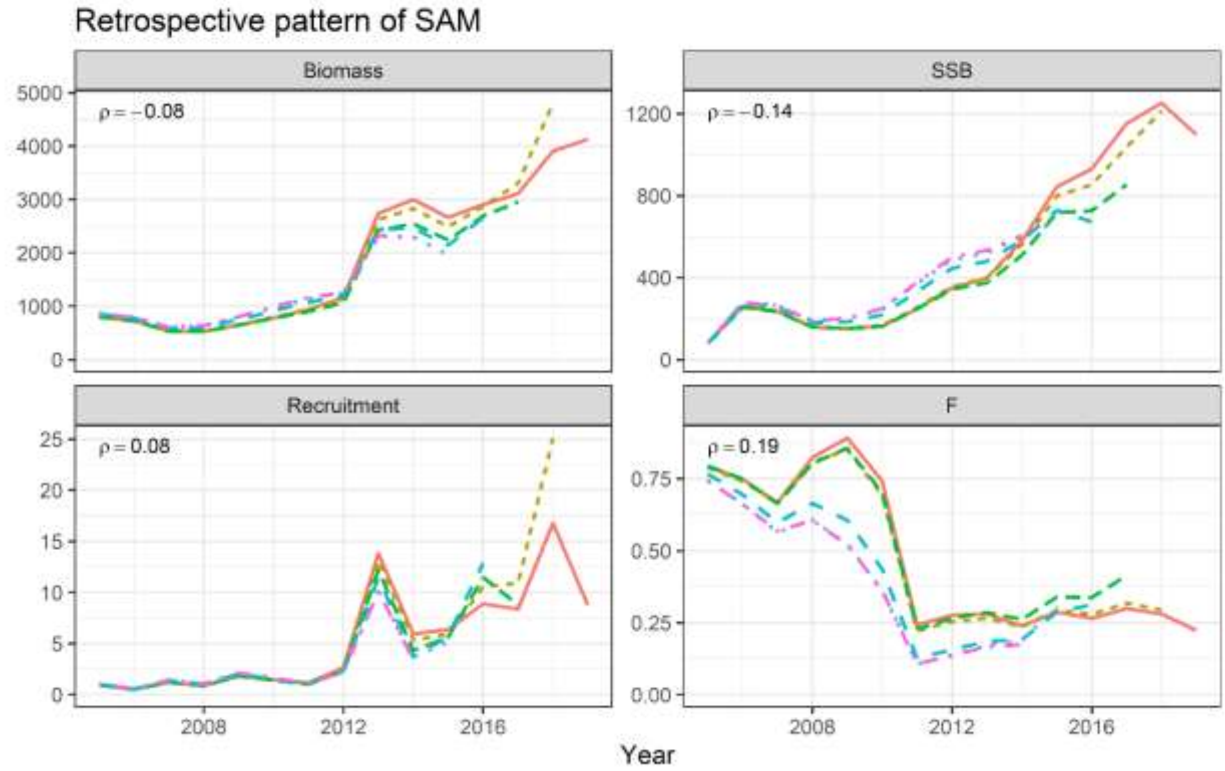

Figure 11: Retrospective pattern of SAM. Mohn's rho is shown in the upper-left side.

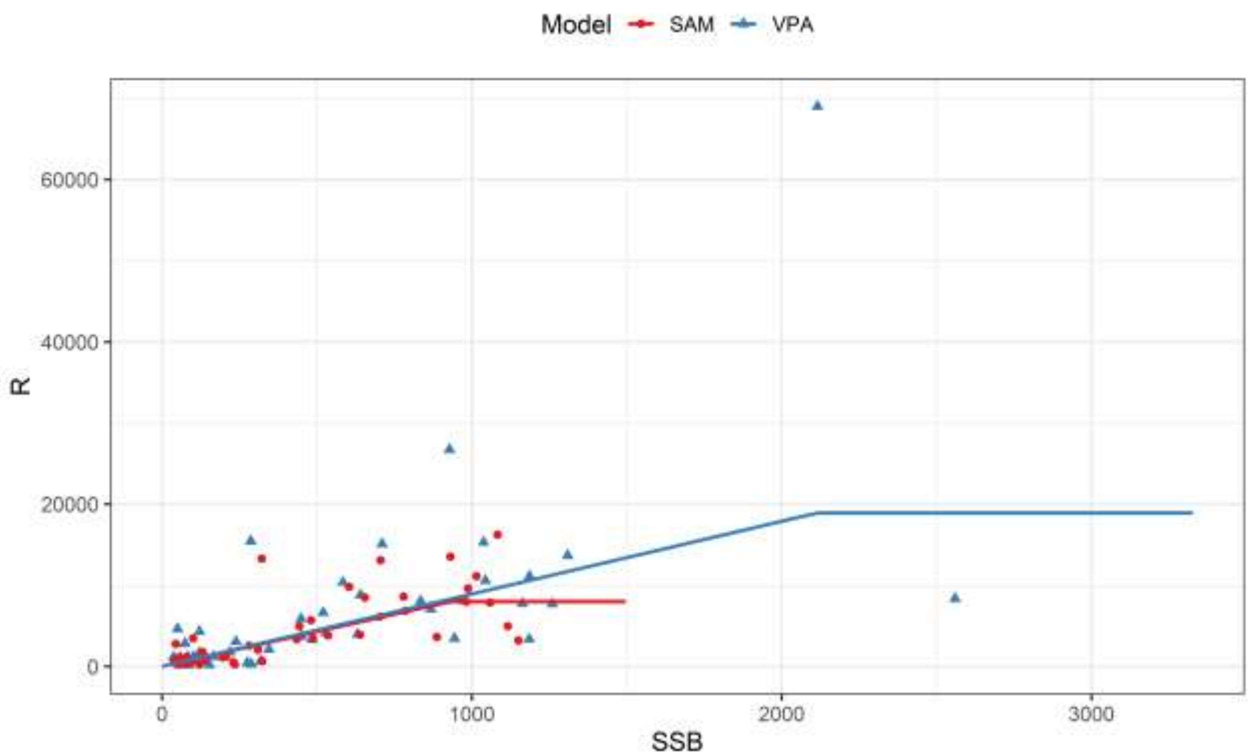

Figure 12: Hockey-Stick stock-recruitment relationship in VPA and SAM.

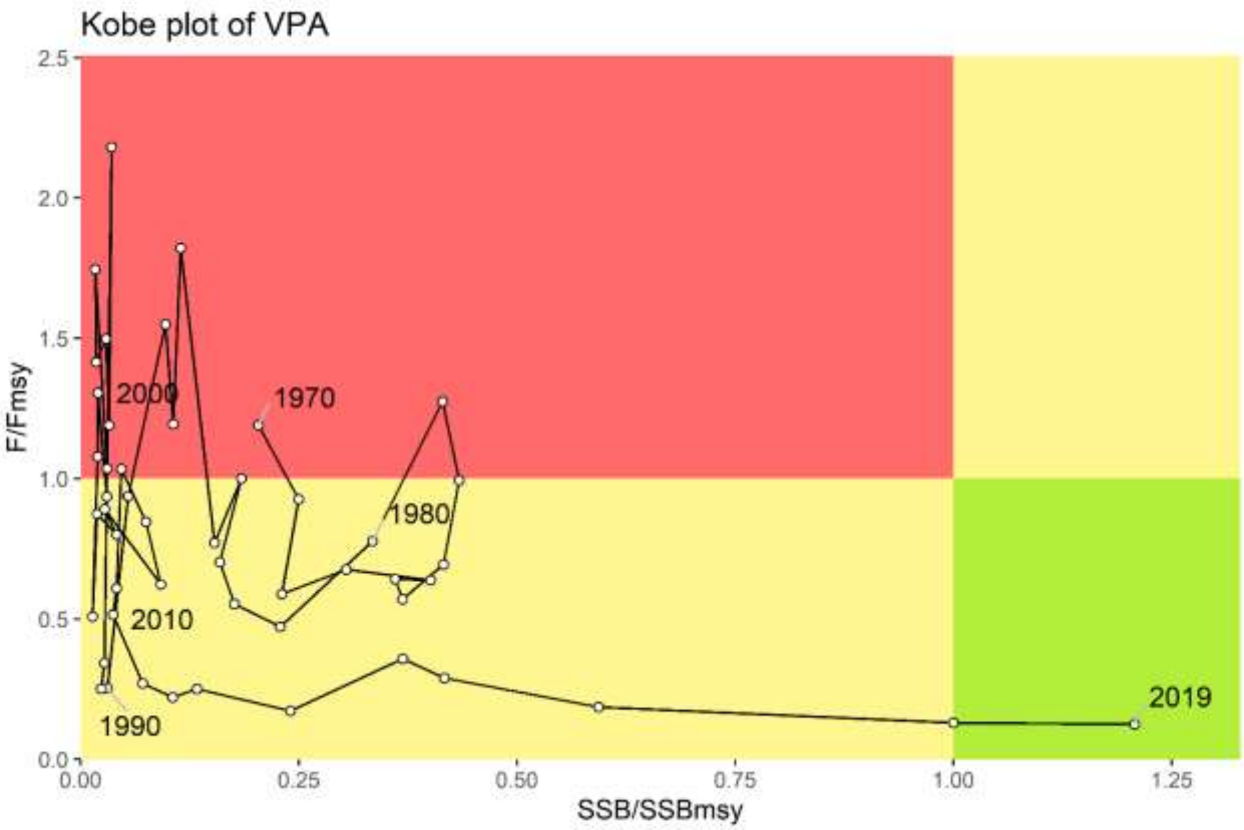

Figure 13: Kobe plot in VPA.

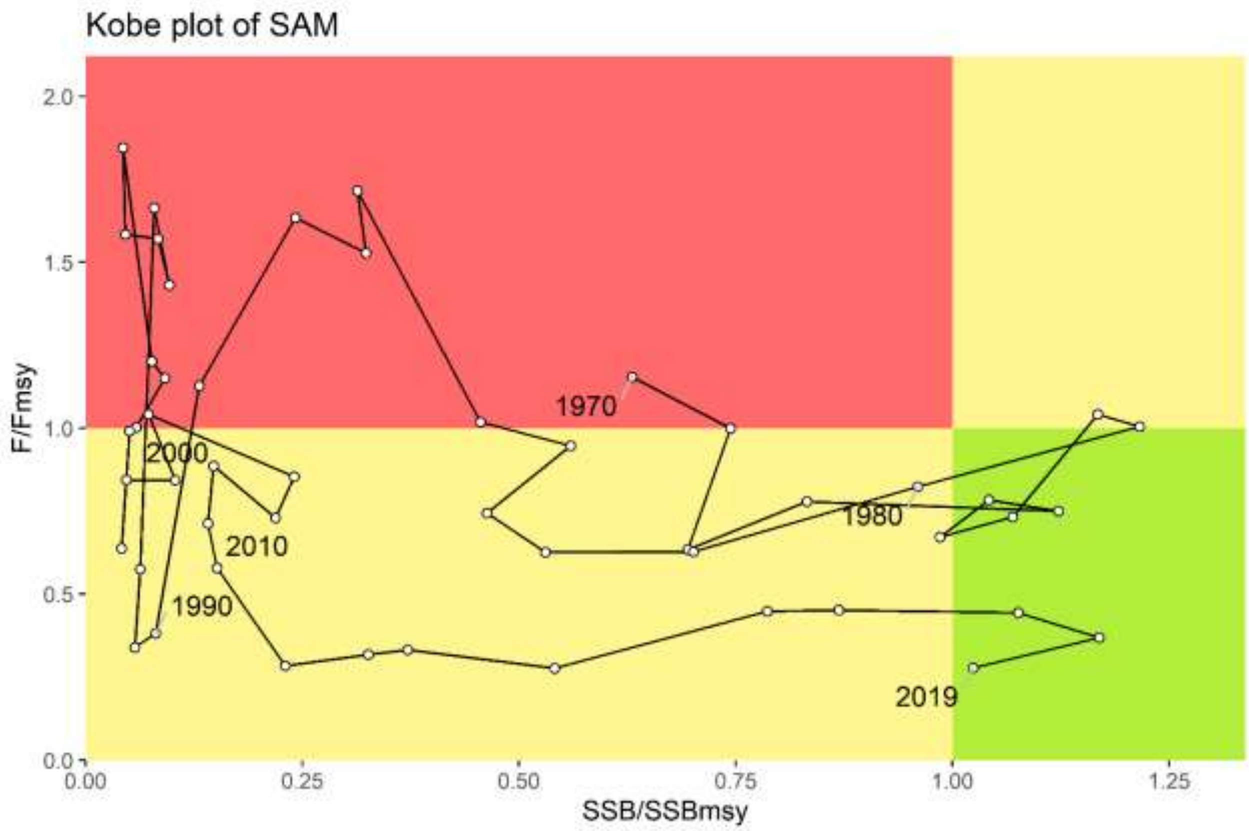

Figure 14: Kobe plot in SAM.

Appendix A: SAM with the Beverton-Holt stock-recruitment relationship

In this appendix we show the results of SAM using the Beverton-Holt (BH) relationship. We could estimate the BH relationship within the stock assessment model in contrast to the base-case in which we used a random-walk (RW) recruitment and then conducted a post-hoc analysis of HS relationship (Fig. 12).

Estimates with the BH relationship in SAM were similar to those with the RW recruitment, while the former estimates of SSB and fishing mortality coefficients were slightly higher and lower, respectively, in recent years (Fig. A1). A serious retrospective bias was not found in this model (Fig. A2). The estimated BH relationship had an almost linear form, i.e., low steepness (Fig. A3), and thus, SSB_{MSY} was estimated to be much higher than the range of SSB estimates (Table 3, Fig. A4). We consider that using the MSY reference points based on the BH relationship is not appropriate in this case, and using the HS relationship may be a better alternative for this stock.

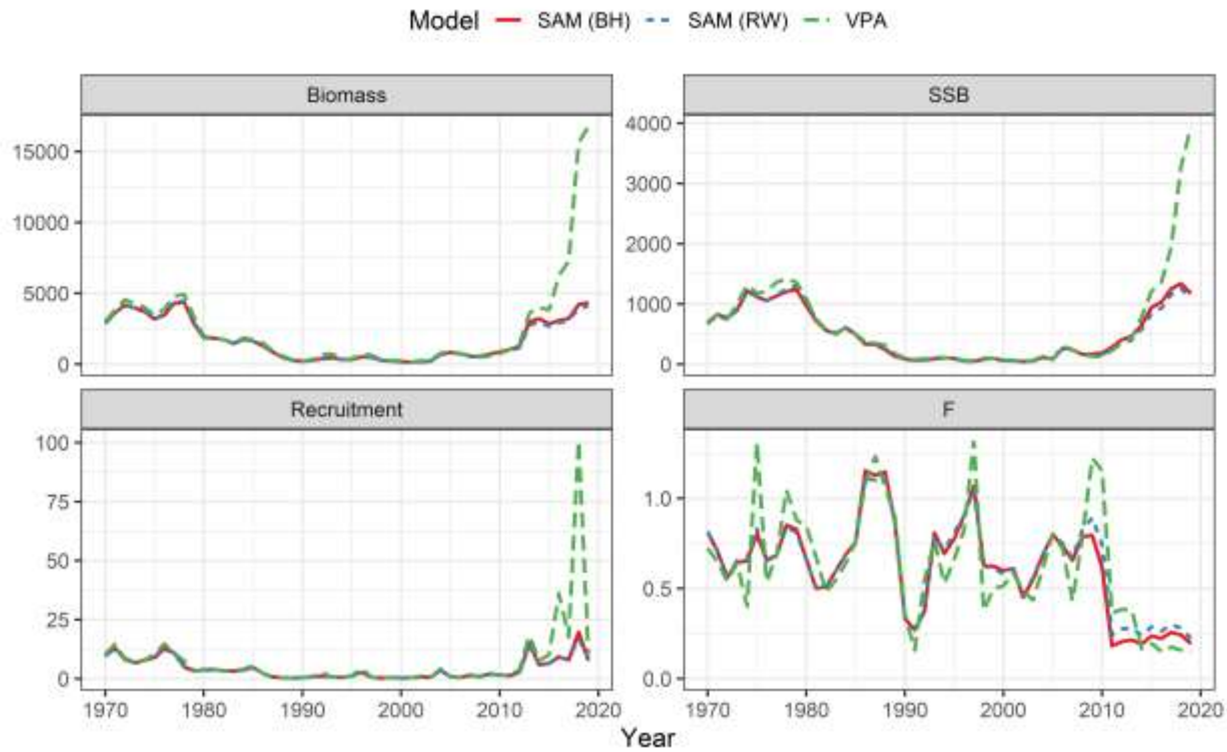

Figure A1: Time series of estimates of total biomass (thousand ton), SSB (thousand ton), recruitment (billion), and average fishing mortality coefficient of SAM with the RW recruitment, SAM with the BH relationship, and VPA.

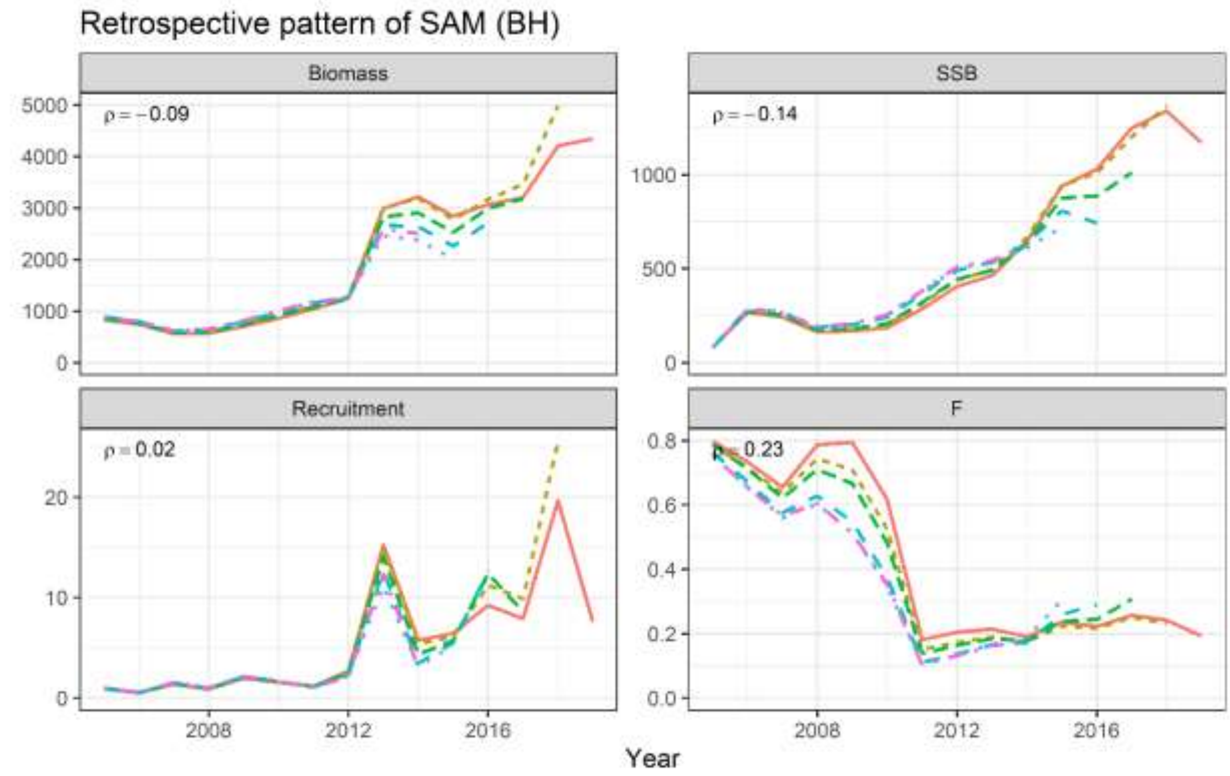

Figure A2: Retrospective pattern of SAM with the BH relationship. Mohn's rho is shown in the upper-left side.

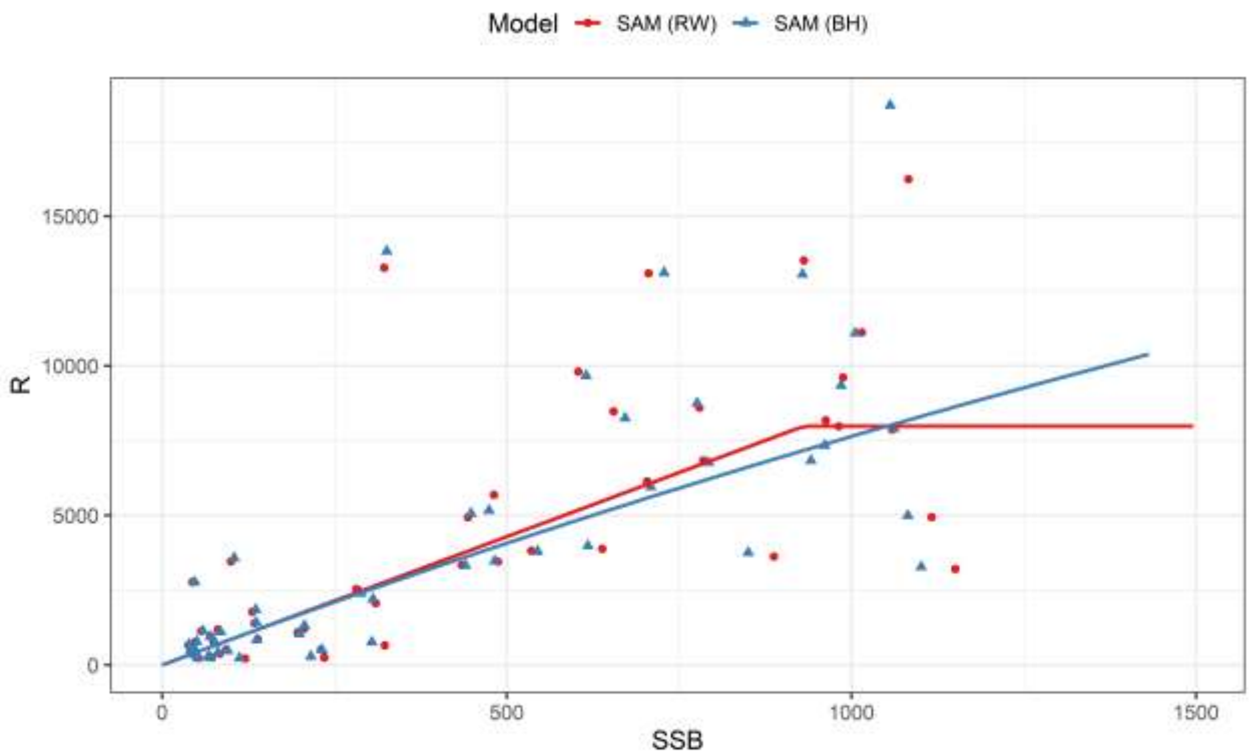

Figure A3: Hockey-Stick relationship in the SAM with the RW relationship and Beverton-Holt stock relationship in the SAM with the BH relationship.

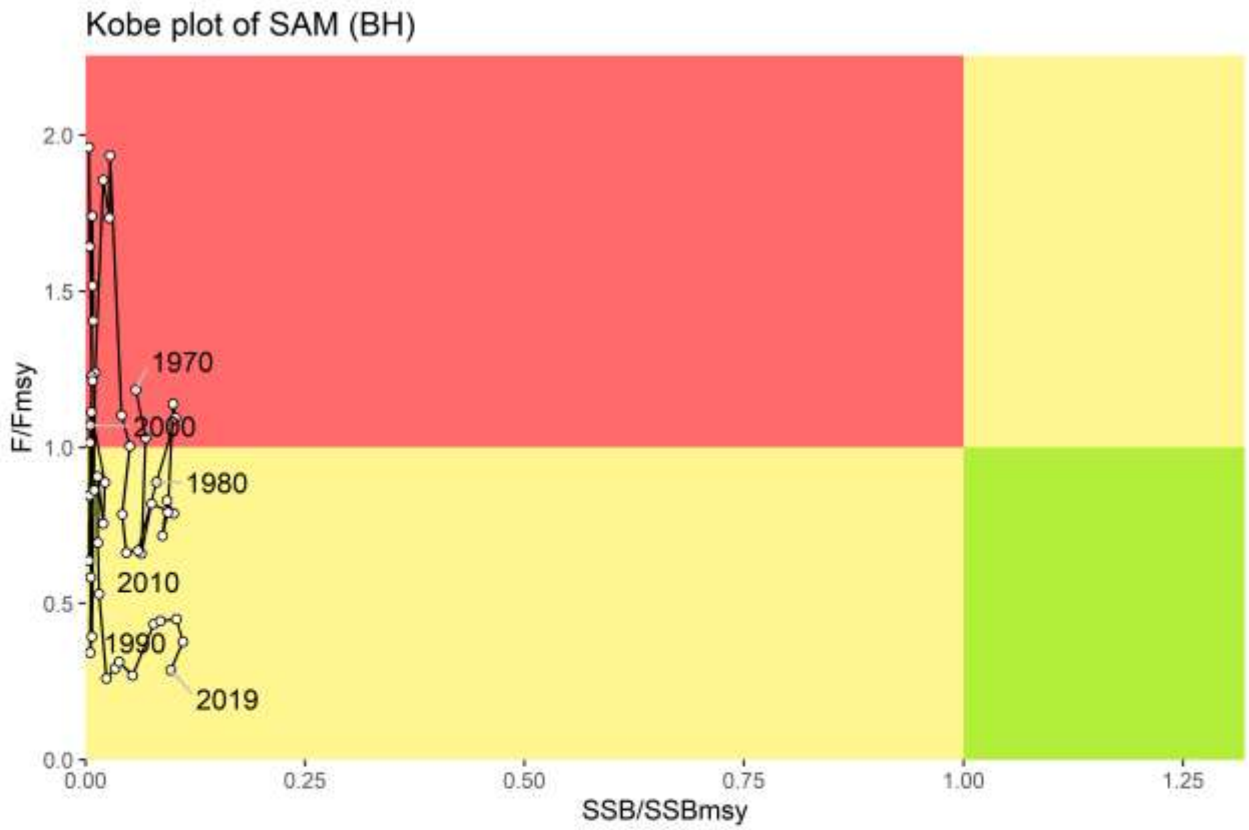

Figure A4: Kobe plot in SAM with the BH relationship.

Appendix B: Models with age-specific natural mortality coefficients

As a sensitivity trial to data uncertainties, we analyzed a case with age-specific natural mortality coefficients ('Gislasson1'). Although Takahashi et al. (2018) did not show M at age 0, we assumed the same value at age 1. M used from age 0 to 6+ is 0.47, 0.47, 0.38, 0.32, 0.28, 0.26, and 0.24.

The abundance estimates in the past years with Gislasson1 were similar to those with M=0.41, whereas the recent estimates in the former case were lower than in the latter especially for VPA (Fig. B1). The average fishing mortality coefficients were slightly higher in the models with Gislasson1 for both VPA and SAM. A large retrospective bias was not observed for VPA (Fig. B2), but the estimates of SAM when removing five-year data was much different from other estimates, suggesting a positive retrospective bias in fishing mortality (Fig. B3).

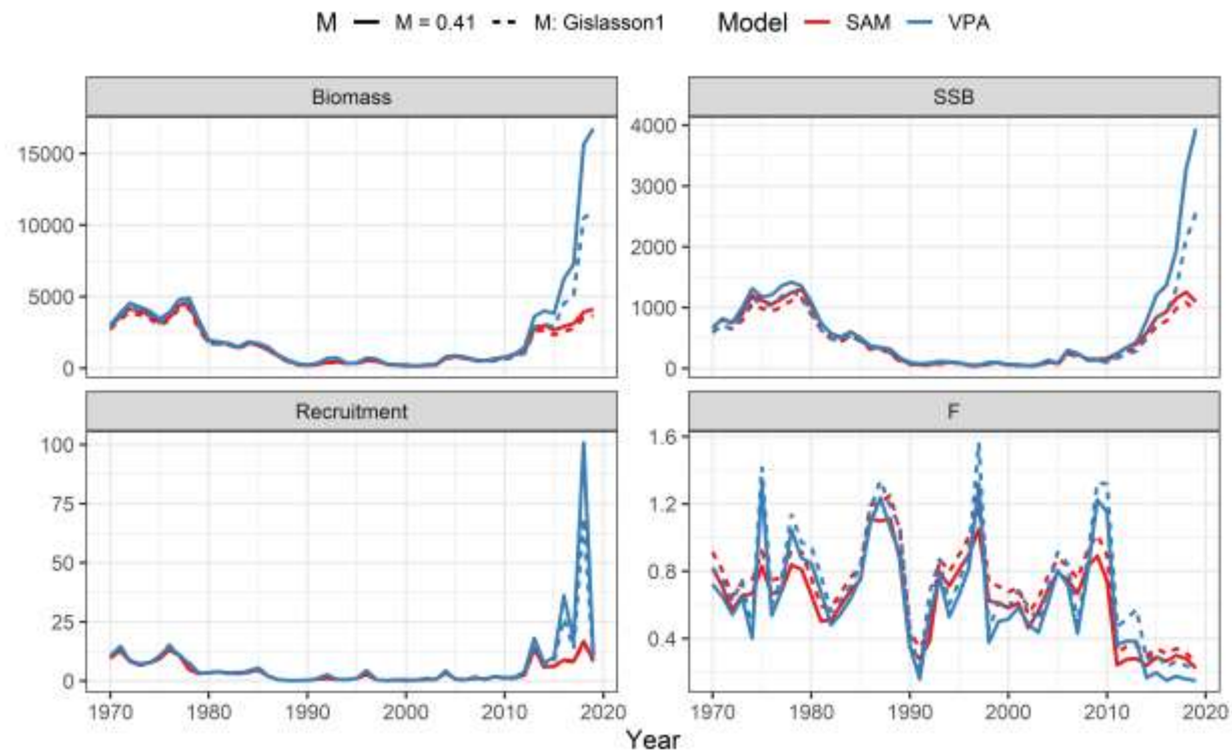

Figure B1: Time series of estimates of total biomass (thousand ton), SSB (thousand ton), recruitment (billion), and average fishing mortality coefficient of SAM and VPA with different natural mortality coefficients (M = 0.41 or Gislasson1).

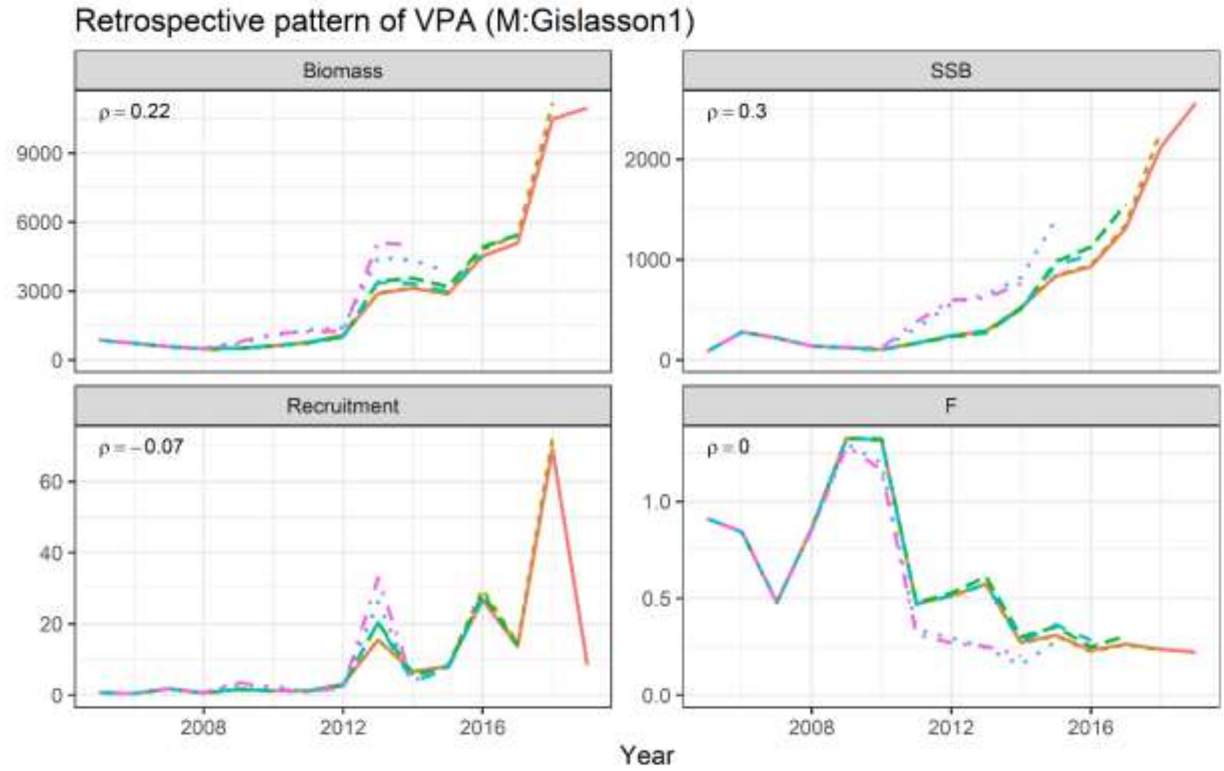

Figure B2: Retrospective pattern of VPA with the age-specific natural mortality coefficients (Gislasson1). Mohn's rho is shown in the upper-left side.

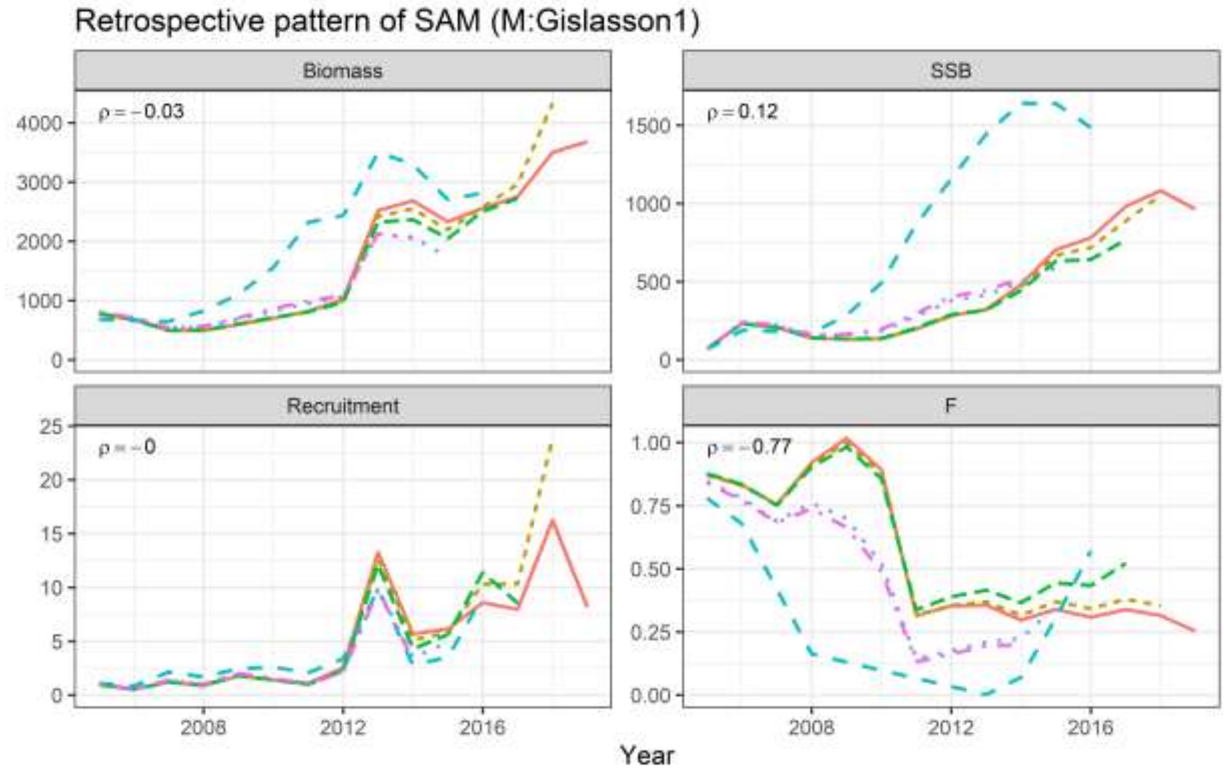

Figure B3: Retrospective pattern of SAM with the age-specific natural mortality coefficients (Gislasson1). Mohn's rho is shown in the upper-left side.